Diffusion-weighted Spin-echo fMRI at 9.4T: Microvascular/tissue Contribution to BOLD Signal Changes

Article *in* Magnetic Resonance in Medicine · December 1999

DOI: 10.1002/(SICI)1522-2594(199911)42:53.0.CO;2-8 · Source: PubMed

4 authors, including:

Phil Lee
University of Kansas Medical Center
69 PUBLICATIONS **2,397** CITATIONS
SEE PROFILE

Afonso C Silva
National Institutes of Health
141 PUBLICATIONS **6,261** CITATIONS
SEE PROFILE

Seong-Gi Kim
Institute for Basic Science, SUngkyunkwan Uni…
222 PUBLICATIONS **21,259** CITATIONS
SEE PROFILE

Magnetic Resonance in Medicine 42:919–928 (1999)

Diffusion-Weighted Spin-Echo fMRI at 9.4 T: Microvascular/Tissue Contribution to BOLD Signal Changes

Sang-Pil Lee, Afonso C. Silva, Kamil Ugurbil, and Seong-Gi Kim*

The nature of vascular contribution to blood oxygenation level dependent (BOLD) contrast used in functional MRI (fMRI) is poorly understood. To investigate vascular contributions at an ultrahigh magnetic field of 9.4 T, diffusion-weighted fMRI techniques were used in a rat forepaw stimulation model. Tissue and blood T_2 values were measured to optimize the echo time for fMRI. The T_2 of arterial blood was 40.8 ± 3.4 msec (mean ± SD; n = 5), similar to the tissue T_2 of 38.6 ± 2.1 msec (n = 16). In comparison, the T_2 of venous blood at an oxygenation level of 79.6 ± 6.1% was 9.2 ± 2.3 msec (n = 11). The optimal spin-echo time of 40 msec was confirmed from echo-time dependency fMRI studies. The intravascular contribution was examined using a graded diffusion-weighted spin-echo echo-planar imaging technique with diffusion weighting factor (b) values of up to 1200 sec/mm^2. Relative BOLD signal changes induced by forepaw stimulation showed no dependence on the strength or direction of the diffusion-sensitizing gradients, suggesting that the large vessel contribution to the BOLD signal is negligible at 9.4 T. However, gradient-echo fMRI performed with bipolar diffusion sensitizing gradients, which suppress intravascular components from large vessels, showed higher percent signal changes in the surface of the brain. This effect was attributed to the extravascular contribution from large vessels. These findings demonstrate that caution should be exercised when interpreting that higher percent changes obtained with gradient-echo BOLD fMRI are related to stronger neural activation. Magn Reson Med 42:919–928, 1999. © **1999 Wiley-Liss, Inc.**

Key words: diffusion; fMRI; spin echo; BOLD; vascular contribution

The blood oxygenation level–dependent (BOLD) effect (1) is the most widely used contrast mechanism for functional MRI (fMRI) (2–4). The BOLD effect is sensitive to venous blood volume and to vessel size and orientation (5–7). These vascular contributions to the BOLD signal, which depend on magnetic field strength as well as on data acquisition methods (8,9), are still poorly understood. To comprehend the nature of vascular contribution, it is important to separate the macrovascular from the microvascular components (10,11). The microvascular or tissue component is defined as coming from capillaries and surrounding tissues, whereas the macrovascular component arises from large venules and veins. The microvascular effect is believed to be close to the neuronal activation site. However, unlike capillaries, large blood vessels are not high in density in the brain (12); thus, functional maps based on the macrovasculature can be significantly distant from the actual site of neural activity. Therefore, it is desirable to minimize the macrovascular contribution.

According to the BOLD model (5,6,13,14), vascular contributions to the BOLD signal are composed of extravascular (EV) and intravascular (IV) effects. The EV contribution from large vessels is linearly dependent on magnetic field strength (B_o), whereas the EV contribution from microvessels increases quadratically with B_o. This suggests that high magnetic fields can increase the relative contribution of the microvascular component to the BOLD signal. The EV component of microvessels contributes to both spin-echo (SE) and gradient-echo (GE) fMRI as a result of dynamic signal averaging induced by water diffusion during an echo time. However, the EV component of large vessels contributes only to GE fMRI, not to SE fMRI, because the 180° RF pulse in SE fMRI can refocus the dephasing effect of the static field inhomogeneity around large vessels (5,6,15,16). These EV effects can not be reduced by applying flow-sensitive bipolar gradients.

The IV signal can be reduced by using bipolar crusher gradients, such as the ones used in diffusion weighting, because fast-moving spins dephase and lose their signal more quickly than static spins. Despite a study using an IV fluorinated blood substitute (17) and recent modeling efforts (18), which have raised the possibility that the IV component may persist even with high diffusion weighting factor (b) values, it is generally accepted that IV signals from large vessels are reduced at b values of 20–30 sec/mm^2 (19). GE fMRI studies using bipolar gradients have been done at 1.5, 3 and 4 T on humans (10,11,20,21). The studies at 1.5 T have shown that most of the BOLD signal increase during visual stimulation is reduced significantly by bipolar gradients, leading to the conclusion that most of the fMRI signal at 1.5 T arises from macrovascular IV effects (10,21). When activation studies were performed at 3 and 4 T, a significant number of pixels remained at b = 200 sec/mm^2, suggesting that a micro- and macrovascular EV and/or microvascular IV BOLD effect coexists with a significant IV contribution associated with the macrovasculature (11,20).

The goal of this work was to investigate the vascular contribution to the BOLD contrast at the ultrahigh magnetic field of 9.4 T with a forepaw somatosensory stimulation paradigm on α-chloralose anesthetized rats (22–25). The T_2 values of blood and tissue were measured to determine an optimal echo time (TE) for the fMRI experiments, and the optimal TE was confirmed with TE dependence fMRI studies. We used a SE sequence with graded diffusion weighting to reveal the contribution of IV spins

Center for Magnetic Resonance Research, Department of Radiology, University of Minnesota Medical School, Minneapolis, Minnesota.

Grant sponsor: National Institutes of Health; Grant numbers: RR08079 and NS38295; Grant sponsor: Whitaker Foundation.

*Correspondence to: Seong-Gi Kim, Ph.D., Center for Magnetic Resonance Research, University of Minnesota Medical School, 2021 Sixth St. SE, Minneapolis, MN 55455. E-mail: kim@cmrr.umn.edu

Received 12 April 1999; revised 8 July 1999; accepted 12 July 1999.

from large vessels to BOLD. Diffusion anisotropy and its effect on the functional activity were examined. We also used a diffusion-weighted GE sequence to determine the contribution from the macrovascular EV component. We found that the major component of the SE BOLD contrast at 9.4 T is of microvascular/tissue origin.

MATERIALS AND METHODS

All NMR measurements were performed with a 9.4-T/31-cm horizontal magnet (Magnex, UK) equipped with an actively shielded, 11-cm-diameter gradient insert operating at a maximum gradient strength of 30 gauss/cm and a rise time of 300 μsec (Magnex, UK) and interfaced to a Unity INOVA console (Varian, CA). A surface coil with a diameter of 1.6 cm was positioned on top of the rat head for in vivo animal studies. Multislice fast low angle shot (FLASH) images were acquired to identify the anatomical structures in the brain and to position the slice of interest in the isocenter of the magnetic field. Magnetic field homogeneity was optimized by either global shimming or volume-localized shimming (FASTMAP) (26) to yield a water spectral linewidth of 16–30 Hz.

Animal Preparation and Stimulation

Male Sprague–Dawley rats weighing 250–300 g were initially anesthetized with 5% isoflurane (Marsam Pharmaceuticals, Cherry Hill, NJ) or 3% halothane (Abbott Labs, North Chicago, IL) in 100% oxygen and intubated for ventilation. The anesthesia gas level was reduced to 2% isoflurane or 1.5% halothane during surgical preparation, and the breathing gas was replaced with a 1:1 mixture of nitrous oxide (N_2O) and oxygen (O_2). Catheters were inserted into both the femoral artery and vein to monitor arterial blood pressure and the arterial and venous blood gases as well as to deliver drugs. The arterial blood pressure and breathing pattern were recorded with a multitrace recorder (AcKnowledge, Biopak, Santa Barbara, CA).

After surgery, isoflurane or halothane anesthesia was discontinued, and 80 mg/kg of α-chloralose was administered by intravenous bolus injection followed by 40 mg/kg every 90 min. The head of the animal was carefully secured in a custom-built restrainer by means of ear pieces and a bite bar to reduce head motion before placement in the magnet. Body temperature was maintained at 37 ± 0.5 °C by using a temperature-controlled water blanket.

Two pairs of needle electrodes were inserted under the skin of the right and left forepaws (between digits 2 and 3 and digits 4 and 5) and connected to a current stimulator (Grass, model S48, West Warwick, RI). Either the right or the left paw was used for each fMRI study. The current flowing underneath the skin of the paw was determined by measuring the voltage across a resistive load connected in series with the needle electrodes. Stimulation parameters were adjusted to elicit the strongest cerebral blood flow response (25). The parameters were a current of 1.5 mA, a pulse duration of 0.3 msec, and a repetition rate of 3 Hz.

Blood and Tissue T_2 Measurements

To determine the optimal TE for maximum contrast-to-noise ratio (CNR), T_2 of brain tissue was measured using a SE EPI sequence (see below) with 12 different TEs between 27 msec and 200 msec and then calculated on a pixel-by-pixel basis using a single-exponential parameter least-square fitting routine. Averaged T_2 values were obtained from regions of interest (ROIs) selected in the somatosensory cortex.

For blood T_2 measurements, 0.5 − 1.0 mL of venous and arterial blood were drawn into heparinized syringes. The blood samples were sealed and placed in a volume coil for T_2 measurements. To minimize the error due to red blood cell precipitation, the samples were agitated immediately before measurement. Conventional SE spectra were obtained at 15 different TEs (1 msec $<$ TE $<$ 120 msec). T_2 of blood samples was calculated with an exponential parameter fitting (VNMR software, Varian) of peak heights of the spectra.

TE Dependence of fMRI

To further optimize the TE of the SE fMRI, fMRI experiments were performed at five TEs ranging from 30 msec to 50 msec. Three TEs were interleaved in each fMRI session. Each experiment had at least one common TE to normalize the animal response difference in different trials. Signal-to-noise ratio (SNR), defined as (mean signal of baseline)/(signal fluctuation of baseline), and relative BOLD signal changes, defined as (signal change)/(mean signal of baseline), were examined in the nine-pixel ROI, chosen from in the active somatosensory cortex area. Data were obtained from 3 animals.

Diffusion-Weighted fMRI

Functional MRI was performed using either a single-shot echo-planar imaging (EPI) technique for low-resolution studies or a two-shot EPI sequence for high-resolution studies. Typical parameters were as follows: data matrix of 64 × 32 for the single-shot EPI and 128 × 64 for the two-shot EPI, field of view (FOV) of 3.0 cm × 1.5 cm, slice-thickness of 2 mm, and repetition time (TR) of 2.5–3.2 sec. Data acquisition was synchronized to the breathing cycle by adjusting the repetition time (TR) to be a multiple of the respiratory period, which was controlled by a pressure-driven ventilator (Kent Scientific, Litchfield, CT). For diffusion-weighted fMRI, a single coronal slice covering the primary somatosensory cortex was selected from multislice data obtained with a GE EPI sequence. The functional MR images were acquired during a paradigm consisting of a 2-min resting period, followed by a 1 min of forepaw stimulation and 2 min of rest. fMRI studies were separated by a rest of at least 10 min.

To obtain SE images with a surface coil, a double SE (27) version of the EPI sequence was implemented by using adiabatic pulses, as shown in Fig. 1. This technique enables us to use a surface coil for RF excitation and detection with optimal sensitivity for SE contrast.

Diffusion-sensitizing bipolar gradients were inserted between the two adiabatic full passage (AFP) radiofrequency (RF) pulses for SE EPI (Fig. 1). If we assume rectangular-shaped gradient pulses, b can be expressed as (28)

$$b = (\gamma \times \delta \times G)^2(\Delta - \delta/3) \quad [1]$$

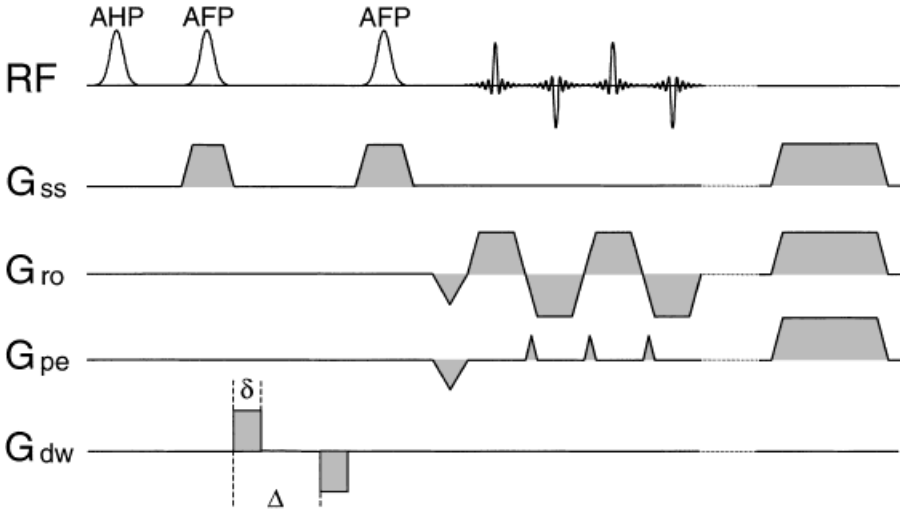

FIG. 1. Pulse sequence diagram for a SE echo-planar imaging technique. Following a non-slice-selective, adiabatic half-passage (AHP) excitation RF pulse, two slice-selective adiabatic full-passage (AFP) RF refocusing pulses were applied. EPI readout followed the spin excitation. For diffusion weighting, bipolar gradients were inserted between two AFP pulses. Gss = slice-selection gradient; Gro = readout gradient; Gpe = phase-encoding gradient; Gdw = diffusion-weighting gradient; δ = gradient duration; Δ = inter-gradient separation.

where γ is the gyromagnetic ratio of a proton, G is a bipolar gradient strength, Δ is the intergradient separation, and δ is the gradient duration. Typical values for the parameters used in this work were Δ = 10 msec, and δ = 5–8 msec. Various b values up to 1200 sec/mm² were achieved by adjusting the gradient strength up to 30 gauss/cm.

b *Value Dependence of Diffusion-Weighted SE fMRI*

To obtain the effect of diffusion weighting on the BOLD signal, G was varied to produce b values of up to 500 sec/mm². The direction of the bipolar gradients was fixed to the longitudinal (z) direction, that is, perpendicular to the coronal slice selected for fMRI. In each study, two or three different b values were interleaved.

Directional Dependence of Diffusion-Weighted SE fMRI

Apparent diffusion coefficients (ADCs) were measured in three different orientations: a radial direction (i.e., dorsal-ventral direction) that is parallel to the large veins in the somatosensory cortex; a tangential direction to the cortical surface in the imaging plane; and a longitudinal (z) direction. Nine different b values up to 500 sec/mm² were used, with Δ = 10 msec and δ = 5 msec. The signal decay due to diffusion weighting can be described as (28)

$$S(b) = S_0 \exp(-b \times \mathrm{ADC}) \qquad [2]$$

where S_0 is the signal intensity obtained at b = 0 sec/mm². ADCs were determined by fitting the average signal intensity within an ROI chosen from the somatosensory cortex to Eq. [2].

To examine the directional dependence of BOLD on the direction of the bipolar gradients, fMRI was performed using the three bipolar gradient orientations described above, with b values varying from 400 sec/mm² to 1200 sec/mm². For each b value, two or three different bipolar gradient directions were interleaved. Subsequently, the order of measurements in different directions was shuffled to avoid possible systematic errors related to the order of data acquisition.

SE Versus GE Diffusion-Weighted fMRI

To investigate EV BOLD effects of large veins, SE and GE diffusion-weighted fMRI data were obtained. Two-shot echo-planar images were obtained with an in-plane resolution of 230 × 230 μm². The GE TE was 16 msec, and the SE TE was 40 msec. Bipolar gradients were applied to produce b values of 100 sec/mm² for SE fMRI and 200 sec/mm² for GE fMRI.

fMRI Data Analysis

Cross-correlation coefficient (CCC) maps were obtained using a boxcar cross-correlation method (29). For quantitative comparisons between different measurements, three different approaches were used: the number of active pixels, the relative percent signal change at an ROI, and the time courses from the ROI.

Active regions consisted of pixels with CCC > 0.5. After a modified Bonferroni correction on 64 × 32 comparisons with a minimum cluster size of 4, cross-correlation value of 0.5, and number of images of 50 or 75, effective P value was $< 1.3 \times 10^{-12}$. The number of active pixels at each b value was normalized by that of the lowest b value for comparison among different trials. To determine relative BOLD signal changes, 9 pixels were chosen from the center of the active area. The ROI had roughly the same area of the forelimb region in the somatosensory cortex, based on the stereotaxic coordinate (30). In some animals, a 25-pixel ROI was also used for comparison with results obtained from the 9-pixel ROI. Averaged percent BOLD signal changes were calculated from the pixels within the ROI, then normalized with the changes at the lowest b value (b value dependence study). Time courses of BOLD signals were obtained within the ROI.

The right side of the image corresponds to the right hemisphere of the rat brain. Data in texts and figures are presented as means ± SD. Student's t-tests were performed to compare differences between measurements. Unless otherwise indicated, differences were considered statistically significant when $P < 0.05$.

RESULTS

Blood and Tissue T_2 Measurements

Figure 2 shows the transverse relaxation rate, $R_2 = 1/T_2$, versus the oxygenation level (Y) of blood with a normal hematocrit level. Blood oxygenation level was altered by changing respiration rate, volume, and the oxygen concentration of the gas mixture. A linear relationship between R_2 and Y ($R^2 = 0.91$, $P < 0.0001$) was observed (Fig. 2). The T_2 of arterial blood obtained at the mean oxygen saturation level of 98.0 ± 1.1% was 40.8 ± 3.4 msec ($n = 5$), similar to the T_2 of the somatosensory cortex, 38.6 ± 2.1 msec ($n = 16$). Meanwhile, the T_2 of venous blood, obtained at the mean oxygen saturation level 79.6 ± 6.1%, was 9.2 ± 2.3 msec ($n = 11$).

TE Dependence of BOLD Contrast

Figure 3a shows the statistical maps overlaid on original SE EPI images obtained at 30-, 40-, and 50-msec TEs. As TE increased, image intensity was reduced by T_2 weighting. As expected, activation was observed only at the contralateral primary somatosensory cortex. The location of the active region was the same in all three images. Foci were consistent with our previous finding (25) and the forelimb area in the stereotaxic coordinates (30). More pixels with high CCC values (yellow color) at TE = 40 msec than at other TEs can be seen in the color maps, suggesting the optimal TE is 40 msec. Average CCC values in the 9-pixel ROI peaked at 40 msec (not shown). Figure 3b plots of the relative signal change and SNR of the BOLD fMRI: BOLD (%) = 133.48 TE + 0.85 ($R^2 = 0.96$). The relative signal changes showed linear dependency on TE. SNR decreased with the TE increase, reflecting the reduced signal intensity due to the T_2 weighting.

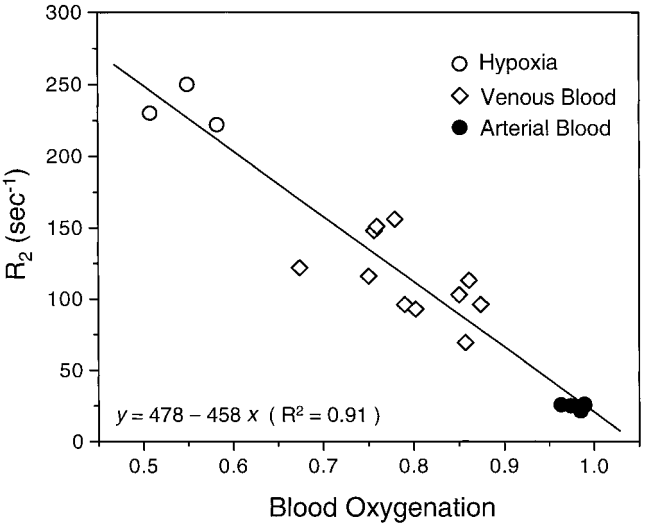

FIG. 2. Oxygenation level dependence of blood T_2. The *y*-axis is R_2, defined as $1/T_2$, and *x*-axis is blood oxygenation (Y). Filled circles at high oxygenation represent arterial blood, and others are from venous blood. Data with open diamonds are from venous blood at normal physiological condition, whereas open circles from venous blood drawn under hypoxic conditions. Solid line graph is a linear regression line ($P < 0.0001$, $R^2 = 0.91$).

b Value Dependence of BOLD Signal

To investigate the vascular contribution to the BOLD signal, a *b* value dependence study was performed. Figure 4a shows the activation maps overlaid on the corresponding BOLD images at two different *b* values. The image intensity at $b = 500$ sec/mm^2 was lower than that at $b = 5$ sec/mm^2 because of overall signal attenuation from the diffusion weighting. Thus, because of the reduced SNR and CNR of the BOLD signal obtained at $b = 500$ sec/mm^2, the size of the active region at $b = 500$ sec/mm^2 was reduced compared with that of $b = 5$ sec/mm^2. These findings were consistently observed in all animals. Table 1 shows the normalized values of BOLD signal intensities, CNR, and sizes of the active areas at various *b* values. The relative BOLD signal intensity decreased as the *b* value increased because of the diffusion weighting effect. The size of the active region decreased with increasing *b* value, reflecting decrease in CNR.

Figure 4b shows the time courses obtained from the ROI in the image on the left. The higher signal fluctuation of the trace at $b = 500$ sec/mm^2 reflects the lower SNR. Clearly, there was no difference in the relative BOLD signal changes at these two different *b* values. Figure 5 shows the overall *b* value dependence of the BOLD signal. Relative BOLD signal changes remained constant, suggesting no IV contributions from large vessels. The same finding was observed when a larger (25-pixel) ROI was used in the calculation.

Directional Dependence of BOLD Signal

To detect large veins in the rat cortex, a high-resolution EPI image with spatial resolution of 150 × 150 × 1000 μm^3, shown in Fig. 6a, was obtained using a two-segmented GE EPI technique with a TE of 15 msec. Because a surface coil was used, only the dorsal part of the cortex was seen. Large veins are clearly seen as black radial lines, indicated by the white arrow in Fig. 6a, because of its shorter T_2^*. The ADC obtained from the somatosensory cortex were (1.01 ± 0.24) × 10^{-3} mm^2/sec in the radial direction ($n = 13$), (0.79 ± 0.19) × 10^{-3} mm^2/sec in the tangential direction ($n = 13$), and (1.10 ± 0.21) × 10^{-3} mm^2/sec in the longitudinal orientation ($n = 10$). The ADC value obtained along the radial orientation was significantly larger than that obtained in the tangential direction ($P = 4.4 \times 10^{-5}$; paired *t*-test), whereas ADC of longitudinal and radial directions did not differ significantly ($P = 0.32$; pooled *t*-test).

To investigate the effect of this diffusion anisotropy on the BOLD signal, we performed fMRI experiments using the same three diffusion gradient orientations. Figure 6b shows diffusion-weighted SE fMRI maps overlaid on EPI images of a rat brain together with an anatomical image showing the ROI. There was no difference in the location or in the size of the active regions at the different orientations. Figure 6c shows the BOLD time courses obtained from the ROI indicated in the bottom right image in Fig. 6b. The magnitude of the BOLD response shows no difference at the three different diffusion orientations (radial direction, 7.1 ± 1.4%; tangential direction, 6.8 ± 1.1%; longitudinal direction, 7.3 ± 1.2%), which is further confirmed by paired Student's *t*-tests on the percent changes: $P = 0.17$ for radial versus tangential, $P = 0.06$ for radial versus longitu-

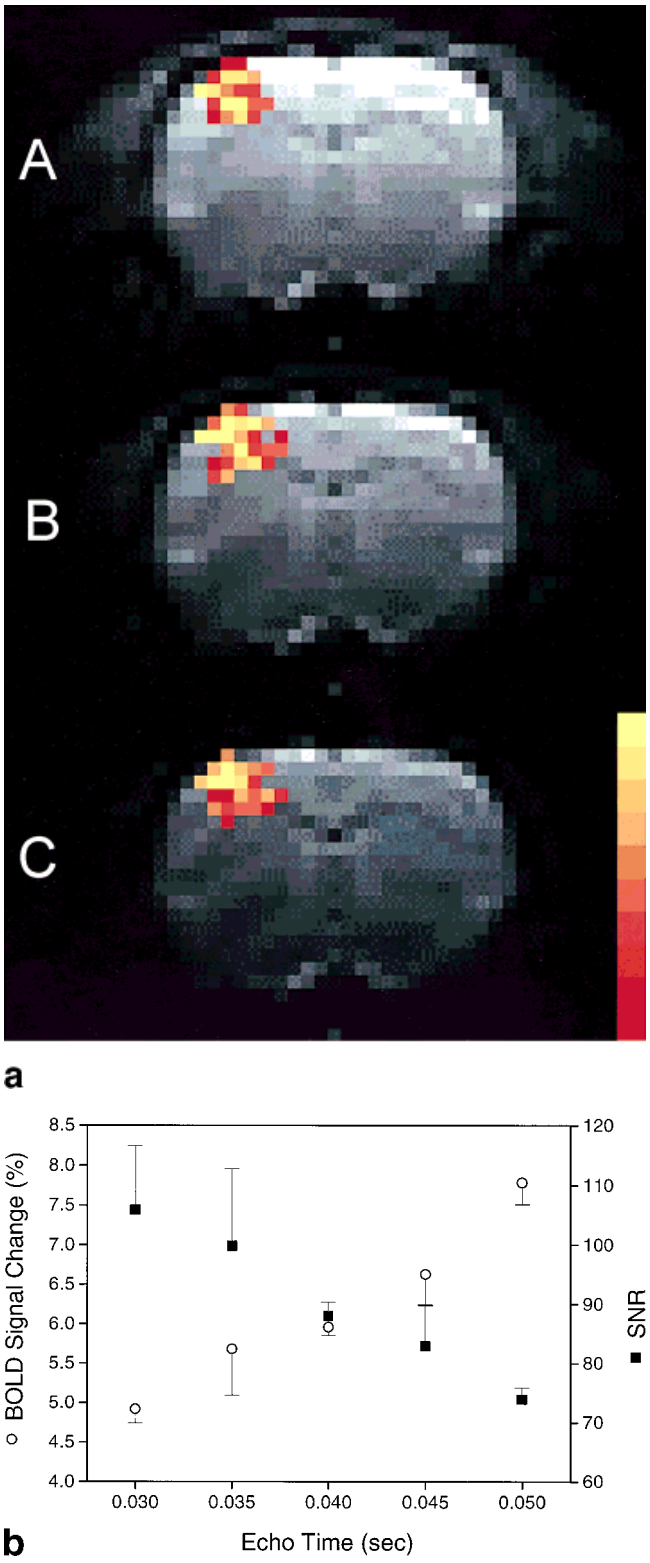

FIG. 3. TE dependence of the SE fMRI. **a:** Statistical maps with TE of 30 msec (A), 40 msec (B), and 50 msec (C) are overlaid on corresponding original BOLD images in a coronal orientation. Color bar represents the cross-correlation values (yellow, CCC ≥ 0.9; red, CCC = 0.5). **b:** Plots of relative BOLD signal changes and SNR vs. TE. Filled squares represent SNR and open circles represent relative BOLD signal changes. Vertical bars indicate standard deviations ($n = 3$). For clarity of the figure, only one side of error bar is displayed. The relative BOLD signal change increases as TE increases, while SNR decreases.

dinal, and $P = 0.06$ for tangential vs. longitudinal directions ($n = 7$).

Comparison of Diffusion-Weighted GE and SE fMRI

To determine EV contributions from large vessels, diffusion-weighted BOLD fMRI was obtained by using a SE sequence with a b value of 100 sec/mm² (TE = 40 msec) and a GE sequence with a b value of 200 sec/mm² (TE = 16 msec). Figure 7 shows statistical maps (left) and percent change maps (right) of SE and GE contrasts obtained during left paw stimulation, overlaid on the original BOLD EPI images. CCC values between 0.5 and 0.9 and percent changes from 3% to 11% were color coded. Only active pixels with CCC > 0.5 were used for the calculation of percent signal changes. In SE fMRI, the area with the highest BOLD percent changes colocalizes with the pixels that present the highest CCC value (top left). However, although the pixels with the highest CCC values in GE fMRI are located in the deep cortical layers, rather than in the cortical surface, the pixels with the highest BOLD percent changes are located along the surface of the cortex (bottom right).

DISCUSSION

Oxygenation Dependence of Blood T_2

At 9.4 T, the T_2 values of arterial and venous blood are 41 msec and 9 msec (at an oxygenation level of 79.6 ± 6.1%), respectively, whereas gray matter T_2 is ~40 ms. As expected, these values are shorter than those reported at lower fields. At 7.0 T, arterial blood T_2 is ~50 msec, whereas the T_2 of venous blood is 15 – 20 msec (31). T_2 values of arterial and venous blood measured using the Hahn echo technique are 100 msec and ~22 msec (at an oxygenation level of 0.7), respectively (32), and T_2 of gray matter is ~ 50 msec at 4.7 T (16). At 1.5 T, arterial and venous blood T_2 values are 254 msec and 181 msec, respectively (33), and T_2 of gray matter is ~90 msec. Note that when SE time is set to T_2 of tissue water, signal contributions from venous blood to T_2-weighted MRI are 0.6, 0.08, and 0.01 times fully relaxed magnetization (M_o) of blood at 1.5, 4.7, and 9.4 T, respectively, whereas tissue contribution is 0.37 times tissue M_o. Hemoglobin (Hb), an endogenous paramagnetic contrast agent in its deoxygenated form, is compartmentalized within red blood cells (RBCs). Thus, deoxygenated hemoglobin generates inhomogeneous field gradients inside and around the RBC. Because the dimension of the RBC (radius: 2 × 5 μm) is small compared with the diffusion distance of water molecules (~8 μm with 1.0×10^{-3} mm²/sec diffusion coefficient and 10 msec diffusion time), the dephasing induced by the local field is irreversible and dynamically averaged (34), which results in a decrease in T_2. This T_2 effect in the presence of deoxyhemoglobin increases quadratically with field strength as expected from dynamic averaging due to diffusion in the presence of field gradients (35).

During increased neural activation, the T_2 of blood itself will change when the deoxyhemoglobin content is altered, leading to signal changes in SE or GE BOLD images. This effect will be present wherever the deoxyhemoglobin content is changed, potentially both in macro- and microvessels. Also, CBV increases during stimulation, result-

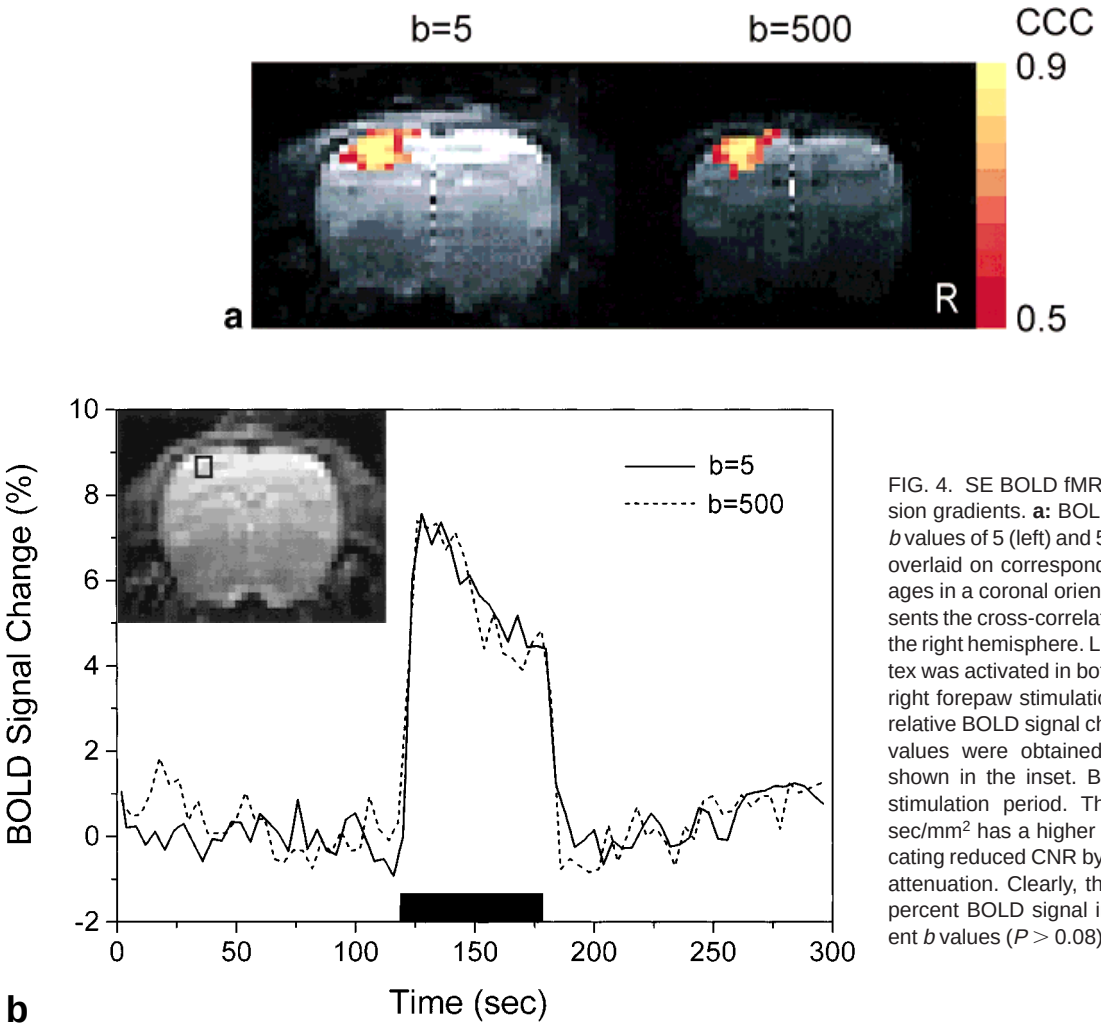

FIG. 4. SE BOLD fMRI dependency on diffusion gradients. **a:** BOLD activation maps with *b* values of 5 (left) and 500 (right) sec/mm^2 are overlaid on corresponding original BOLD images in a coronal orientation. Color bar represents the cross-correlation values. R indicates the right hemisphere. Left somatosensory cortex was activated in both functional maps with right forepaw stimulation. **b:** Time courses of relative BOLD signal change at two different *b* values were obtained from a 9-pixel ROI, shown in the inset. Black bar indicates the stimulation period. The trace of $b = 500$ sec/mm^2 has a higher signal fluctuation, indicating reduced CNR by reduced overall signal attenuation. Clearly, there is no difference in percent BOLD signal increases at two different *b* values ($P > 0.08$).

ing in the increase of the partial blood volume fraction in a given voxel. The signal intensity can be described by

$$S(TE)/S_0 = (1 - \nu)\, e^{-TE/T_2(tissue)} + \nu\, e^{-TE/T_2(blood)} \quad [3]$$

Table 1
Diffusion Weighting Dependence of BOLD Signal Intensity, CNR, and Size of the Activated Area*

b[a] (sec/mm^2)	Normalized BOLD[b]	Normalized CNR[c]	No. of active pixels[d]	No. of observations[e]
3.9 ± 1.9	1.00	1.00	1.00	15
28.3 ± 3.9	0.97 ± 0.05	0.88 ± 0.14	0.96 ± 0.37	12
128.6 ± 48.8	0.85 ± 0.05	0.98 ± 0.27	1.06 ± 0.15	7
476.9 ± 43.9	0.61 ± 0.04	0.77 ± 0.19	0.70 ± 0.27	13

*Data were obtained from 9 animals. All values are means ± SD.
[a]Average *b* values over 0–5, 20–30, 100–200, and 400–500 blocks.
[b]BOLD signal was normalized by the signal obtained at the lowest *b* values.
[c]CNR was normalized by the CNR at the lowest *b* value.
[d]Number of active pixels is counted from the pixels with CCC >0.5, then normalized with the number at the lowest *b* value.
[e]Number of measured paws.

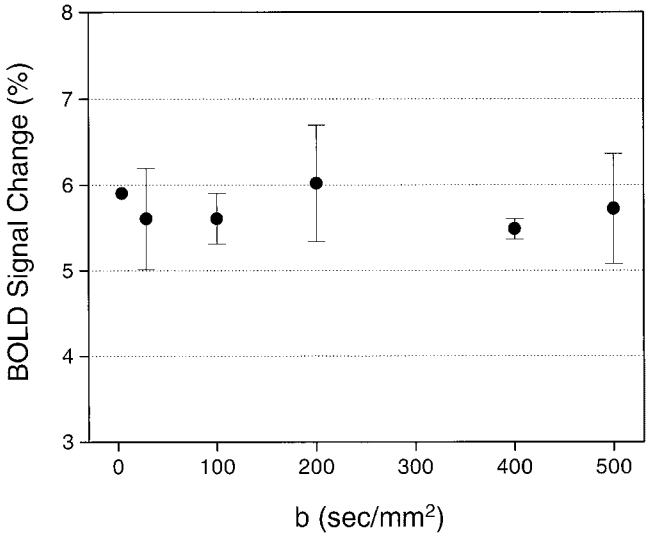

FIG. 5. Normalized SE BOLD-based fMRI signal change versus *b* value. An average BOLD signal change was 5.9% at TE = 40 msec. Vertical bars indicate standard deviations. The BOLD signal does not depend on the diffusion weighting, indicating negligible vascular contribution.

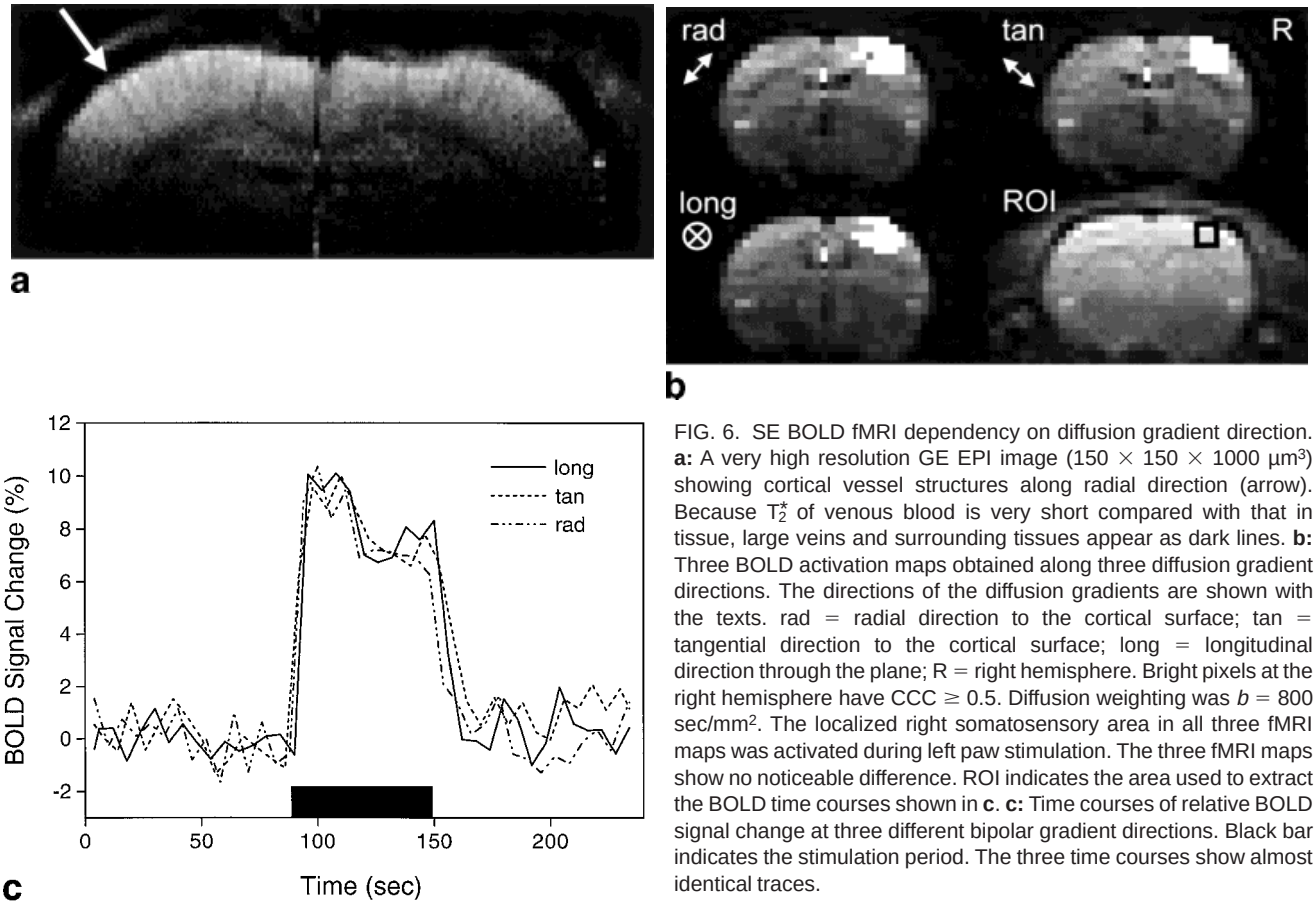

FIG. 6. SE BOLD fMRI dependency on diffusion gradient direction. **a:** A very high resolution GE EPI image (150 × 150 × 1000 μm^3) showing cortical vessel structures along radial direction (arrow). Because T_2^* of venous blood is very short compared with that in tissue, large veins and surrounding tissues appear as dark lines. **b:** Three BOLD activation maps obtained along three diffusion gradient directions. The directions of the diffusion gradients are shown with the texts. rad = radial direction to the cortical surface; tan = tangential direction to the cortical surface; long = longitudinal direction through the plane; R = right hemisphere. Bright pixels at the right hemisphere have CCC ≥ 0.5. Diffusion weighting was b = 800 sec/mm^2. The localized right somatosensory area in all three fMRI maps was activated during left paw stimulation. The three fMRI maps show no noticeable difference. ROI indicates the area used to extract the BOLD time courses shown in **c**. **c:** Time courses of relative BOLD signal change at three different bipolar gradient directions. Black bar indicates the stimulation period. The three time courses show almost identical traces.

where ν is the total blood volume fraction, and T_2(tissue) and T_2(blood) are the transverse relaxation times of tissue and blood, respectively. At 9.4 T, the increase in ν will decrease the BOLD signals for a given TE because T_2(tissue) is much longer than T_2(blood). However, at 1.5T, an increase in arterial and/or venous blood volume fraction will increase BOLD signal because T_2(tissue) is shorter than T_2(blood). This partial volume component of BOLD is relatively small compared with T_2 and susceptibility changes, because ν is about 0.05 at most (36).

Vascular Contribution to BOLD

SE time was optimized by using various SE times in fMRI. We found, as expected, that the TE of 40 msec gave the highest CNR. Thus, we used a TE of 40 msec for further fMRI studies. Assuming the venous blood volume to be $\sim 2 - 3\%$ of the total brain volume (12,36) and no susceptibility effect around blood vessels, the contribution of venous blood to the BOLD signal at 9.4 T is estimated to be only $0.10 - 0.15\%$ compared with the tissue signal at TE = 40 msec. The remaining IV contribution can be further suppressed by bipolar gradients.

To understand the behavior of moving spins under the presence of a gradient, the dephasing effect is considered in a group of moving spins with a constant velocity (v) under the bipolar gradients along the direction of flow. Assuming plug flow, the phase shift induced by the two opposite gradients is described by

$$\phi = \gamma \int_0^{\delta} G(x + vt)\, dt - \gamma \int_{\Delta}^{\Delta+\delta} G(x + vt)\, dt = \gamma G v \delta \Delta \quad [4]$$

where x is the position of the spins. However, plug flow is unlikely to occur in vivo because of a small vessel dimension and the high viscosity of blood (34). Laminar or turbulent flow is observed in vivo, which has higher velocity at the center of vessels and slower velocity near vessel walls. Thus, within blood vessels, flow is not uniform. Furthermore, the blood vessels may change directions within a voxel, and there may be several different blood vessels with different flow rates and/or different orientations relative to the gradient directions (37). Because the blood signal detected from the voxel will have contributions from all vessels within the voxel, the net result can be signal cancellation due to dephasing of flowing spins. Therefore, bipolar gradients can very effectively suppress flowing spins in blood vessels. Although the efficiency of signal suppression with respect to blood vessel size is controversial, it is widely accepted that higher bipolar gradients decrease macrovascular contributions (10,19). Because large venous vessels induce larger BOLD signal changes than smaller vessels, the relative BOLD signal change will decrease when the b value increases if macrovascular IV contribution is significant. In

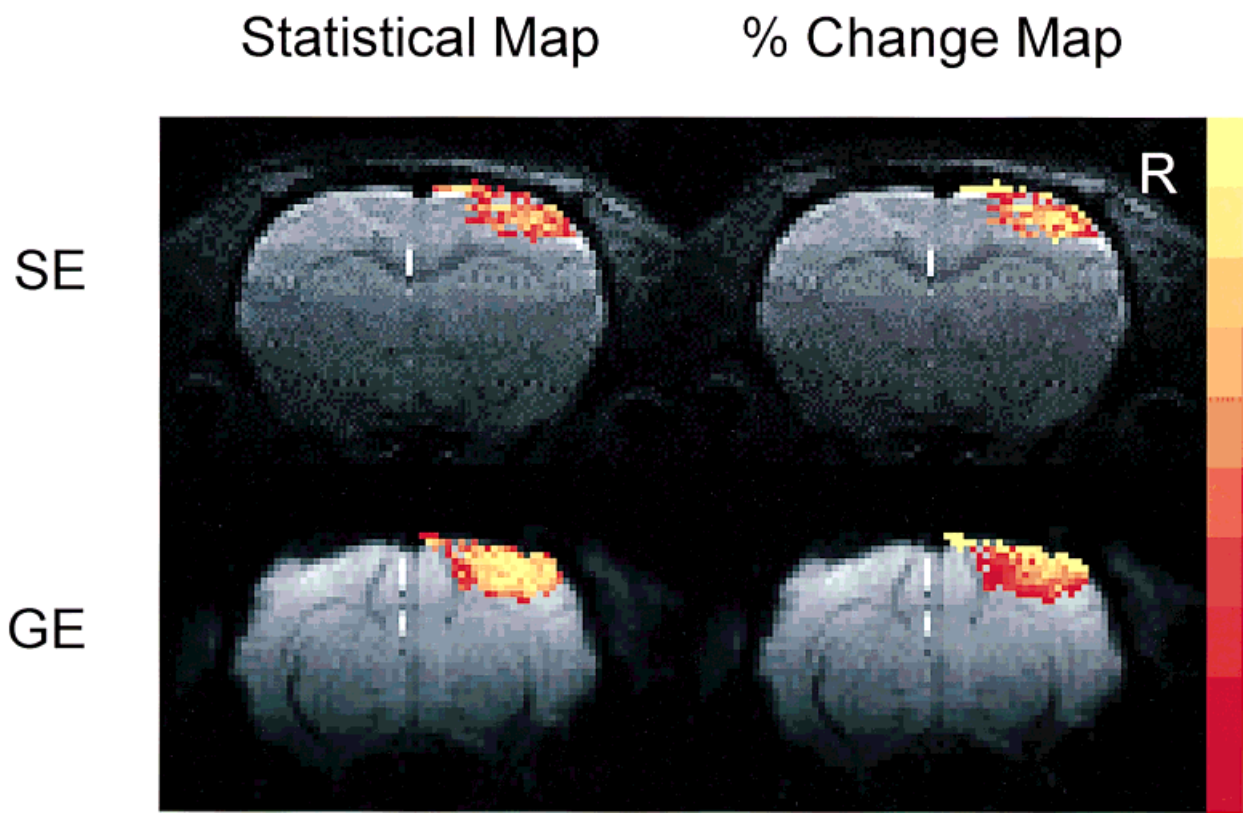

FIG. 7. Comparison between GE and SE BOLD fMRI. BOLD statistical maps are overlaid on two segmented EPI images with resolution = 230 × 230 × 2000 μm^3 and TE = 16 msec (GE) or TE = 40 msec (SE). SE images shown in the top row are diffusion weighted with b = 100 sec/mm^2, and GE images shown in the bottom row with b = 200 sec/mm^2. Left column indicates CCC maps and right column relative BOLD signal change maps. Color bar indicates CCCs between 0.5 and 0.9 and BOLD percentage change between 3% and 11%. Both CCC maps of SE and GE images present high CCC values in the deep layers of the somatosensory cortex. However, in the BOLD percent signal increase maps, the GE activation map shows high signal increase at the surface of the brain, where large superficial veins are located. The BOLD percent increase map shown in the SE image (top right) agrees with the corresponding CCC map (top left).

our diffusion-weighted ^{19}F NMR study using IV perfluorocarbon, arterial blood was effectively eliminated, whereas venous blood was not significantly reduced with bipolar gradients with b value of 200 sec/mm^2 (unpublished observations, T. Q. Duong and S.-G. Kim).

We did not observe any dependence of the relative BOLD signal increase on b values. This result suggests that IV signals from large vessels are not significant in SE fMRI at 9.4 T. The very short T_2 values of venous blood accounts for the above observations because the venous blood signal is strongly attenuated by the use of an EPI sequence with a long TE. Compared with lower magnetic field results (10,21), high magnetic field strengths have the advantage of making the BOLD signal better confined mainly to the microvasculature and tissue.

When the b value increases, the number of active pixels decreases due to the decrease of SNR, as shown in Table 1. Careful comparison between signals with different SNR or CNR needs to be made, because CNR and SNR can affect the statistical significance level of signal change. The CNR directly influence the CCC, whereas the SNR indirectly affects CCC because SNR is a measure of signal intensity versus signal fluctuation during control periods. Diffusion weighting does not decrease signal fluctuation but decreases the signal intensity and the signal difference between a control state and a stimulation state, which results in the decrease of SNR and CNR. The size of an activated area determined by a threshold in CCC will decrease with SNR reduction due to diffusion weighting.

Directional Dependence of BOLD Signal

We observed diffusion anisotropy in the cortical area (gray matter), which is consistent with previous findings (38). The previous study showed diffusion anisotropy between medial-lateral and dorsal-ventral directions. Our study clearly demonstrates that the radial direction has higher apparent diffusion rates than the tangential direction within the imaging slice. However, this anisotropy did not decrease after the animals were sacrificed, suggesting that the blood flow in the large radial vessels, shown in the high resolution T_2^* weighted image of Fig. 6a, is not the major source of diffusion anisotropy. The anisotropy is probably related to neuronal fiber directions.

We have shown that the direction of diffusion weighting has no correlation with BOLD signal changes during forepaw stimulation, suggesting that diffusion anisotropy does not play a role in the BOLD effects. This can be partly explained by the small b values of up to 1200 sec/mm^2 and the short diffusion time used in this study.

Comparison of SE and GE BOLD fMRI

Most fMRI studies use T_2^*-based GE techniques, which have higher contrast than T_2-based SE techniques (5). Thus, T_2^*-weighted BOLD techniques have been used in high-resolution studies. To obtain accurate high-resolution functional maps, it is crucial to remove large vessel contributions. At 9.4 T, because the T_2 of venous blood is <10 msec, the IV component of high-resolution GE images was minimized by the relatively long TE (16 msec). Furthermore, any remaining IV component was further attenuated by bipolar gradients. Active foci in the statistical map are located in the deep layers of the cortex and agree well between SE and GE BOLD maps. These findings are consistent with our previous cerebral blood flow (CBF) (25) and synaptic activity studies (39) showing agreements among foci of the active pixels in GE BOLD CCC maps, CBF CCC maps, and synaptic activity maps obtained using Mn^{2+} infusion as a contrast agent.

To determine the magnitude of activation, it is necessary to use relative signal changes, rather than statistical values. A CCC is the relative significance level of a signal change to the noise fluctuation, obtained by matching the signal time course to a hypothesized waveform such as a block function. Therefore, the CCC can be used to distinguish an active area from a nonactive area but cannot differentiate the degree of activation. On the contrary, the relative signal change, defined by the fractional signal difference between stimulation and resting state, can grade the activation and determine the highest activation area only if microvascular/tissue component dominates. If the macrovascular contribution is suppressed, then the combination of the CCC method and the relative signal change method can colocalize the most active area, which is the case for SE BOLD. In GE fMRI, the highest percent signal change takes place near the edge of the brain, because the EV component from large vessels cannot be suppressed by a GE sequence. Areas near large veins at the edge of the brain are sensitive to cardiac pulsation and have lower signals than tissue because of the susceptibility effect. Therefore, their statistical values are lower than those of deep tissue area, even though the percent changes are higher. The large vessel contribution in GE BOLD signal change was not removed but in fact dominated even when bipolar gradients were used. These observations imply that GE fMRI is susceptible to the large vessel contribution even with a relatively long TE and diffusion weighting gradients.

In conclusion, we have shown that only microvascular/tissue regions contribute to the SE BOLD signal at 9.4 T. This result is strongly supported by the independence of our fMRI data on graded diffusion weighting and different diffusion weighting directions. To obtain microvascular/tissue–based fMRI, high magnetic fields are preferable, because the microvascular contribution dominates and the BOLD signal changes are strong enough to allow a SE sequence to be used. The IV signal from large vessels can be minimized by diffusion weighting and by using a long TE relative to the T_2 of venous blood. Therefore, the combination of SE methods and diffusion weighting at high magnetic fields can make it possible to obtain very high resolution functional MR images devoid of contributions from large vessels.

ACKNOWLEDGMENTS

The authors thank Hellmut Merkle for hardware support. The 9.4-T facility was funded partly by the Keck Foundation.

REFERENCES

1. Ogawa S, Lee T-M, Kay AR, Tank DW. Brain magnetic resonance imaging with contrast dependent on blood oxygenation. Proc Natl Acad Sci USA 1990;87:9868–9872.
2. Ogawa S, Tank DW, Menon R, Ellermann JM, Kim S-G, Merkle H, Ugurbil K. Intrinsic signal changes accompanying sensory stimulation: functional brain mapping with magnetic resonance imaging. Proc Natl Acad Sci USA, 1992;89:5951–5955.
3. Kwong KK, Belliveau JW, Chesler DA, Goldberg IE, Weisskoff RM, Poncelet BP, Kennedy DN, Hoppel BE, Cohen MS, Turner R, Cheng H-M, Brady TJ, Rosen BR. Dynamic magnetic resonance imaging of human brain activity during primary sensory stimulation. Proc Natl Acad Sci USA 1992;89:5675–5679.
4. Bandettini PA, Wong EC, Hinks RS, Rikofsky RS, Hyde JS. Time course EPI of human brain function during task activation. Magn Reson Med 1992;25:390–397.
5. Ogawa S, Menon RS, Tank DW, Kim S-G, Merkle H, Ellermann JM, Ugurbil K. Functional brain mapping by blood oxygenation level-dependent contrast magnetic resonance imaging. Biophys J 1993;64:800–812.
6. Weisskoff RM, Zuo CS, Boxerman JL, Rosen BR. Microscopic susceptibility variation and transverse relaxation: theory and experiment. Magn Reson Med 1994;31:601–610.
7. Ogawa S, Menon RS, Kim S-G, Ugurbil K. On the characteristics of functional magnetic resonance imaging of the brain. Annu Rev Biophys Biomol Struct 1998;27:447–474.
8. Frahm J, Merboldt K-D, Hanicke W, Kleinschmidt A, Boecker H. Brain or vein—oxygenation or flow? On signal physiology in functional MRI of human brain activation. NMR Biomed 1994;7(1/2):45–53.
9. Kim S-G, Hendrich K, Hu X, Merkle H, Ugurbil K. Potential pitfalls of functional MRI using conventional gradient-recalled echo techniques. NMR Biomed 1994;7(1/2):69–74.
10. Song AW, Wong EC, Tan SG, Hyde JS. Diffusion-weighted fMRI at 1.5T. Magn Reson Med 1996;35:155–158.
11. Menon RS, Hu X, Adriany G, Andersen P, Ogawa S, Ugurbil K. Comparison of SE-EPI, ASE-EPI and conventional EPI applied to functional neuroimaging: the effect of flow crushing gradients on the BOLD signal. In: Proc of the SMRM 2nd Scientific Meeting, San Francisco, 1994. p 622.
12. Johnson PC, editor. Peripheral circulation. New York: Wiley; 1978.
13. Bandettini PA, Wong EC. Effects of biophysical and physiologic parameters on brain activation–induced R2* and R2 changes: simulations using a deterministic diffusion model. Int J Imaging Systems Technol 1995;6:133–152.
14. Kennan RP, Zhong J, Gore JC. Intravascular susceptibility contrast mechanisms in tissues. Magn Reson Med 199431:9–21.
15. Bandettini PA, Wong EC, Jesmanowicz A, Hinks RS, Hyde JS. Spin-echo gradient-echo EPI of human brain activation using BOLD contrast: a comparative study at 1.5 T. NMR Biomed 1994;7(1/2):12–20.
16. van Zijl PC, Eleff SM, Ulatowski JA, Oja JM, Ulug AM, Traystman RJ, Kauppinen RA. Quantitative assessment of blood flow, blood volume and blood oxygenation effects in functional magnetic resonance imaging. Nature Med 1998;4:159–167.
17. Neil JJ, Ackerman JJH. Detection of pseudodiffusion in rat brain following blood substitution with perfluorocarbon. J Magn Reson 1992;97:194–201.
18. Henkelman R, Neil J, Xiang Q-S. A quantitative interpretation of IVIM measurements of vascular perfusion in the rat brain. Magn Reson Med 1994;32:464–469.
19. Silva A, Williams D, Koretsky A. Evidence for the exchange of arterial spin-labeled water with tissue water in rat brain from diffusion-sensitized measurements of perfusion. Magn Reson Med 1997;38:232–237.
20. Song AW, Wong EC, Jezmanowicz A, Tan SG, Hyde JS. Diffusion weighted fMRI at 1.5 T and 3 T. In: Proc of the SMRM 3rd Scientific Meeting, Nice, France, 1995. p 457.

21. Boxerman JL, Bandettini PA, Kwong KK, Baker JR, Davis TL, Rosen BR, Weisskoff RM. The intravascular contribution to fMRI signal change: Monte Carlo modeling and diffusion-weighted studies in vivo. Magn Reson Med 1995;34:4–10.
22. Ueki M, Linn F, Hossmann K-A. Functional activation of cerebral blood flow and metabolism before and after global ischemia of rat brain. J Cereb Blood Flow Metab 1988;8:486–494.
23. Gyngell ML, Bock C, Schmitz B, Hoehn-Berlage M, Hossmann K-A. Variation of functional MRI signal response to frequency of somatosensory stimulation in α-chloralose anesthetized rats. Magn Reson Med 1996;36:13–15.
24. Hyder F, Behar K, Martin M, Blamire A, Shulman R. Dynamic magnetic resonance imaging of the rat brain during forepaw stimulation. J Cereb Blood Flow Metab 1994;14:649–655.
25. Silva AC, Lee S-P, Yang G, Iadecola S, Kim S-G. Simulataneous BOLD and perfusion functional MRI during forepaw stimulation in rat. J Cereb Blood Flow Metab 1999;19:871–879.
26. Gruetter R. Automatic, localized in vivo adjustment of all first- and second-order shim coils. Magn Reson Med 1993;29:804–811.
27. Schupp DG, Merkle H, Ellermann JM, Ke Y, Garwood M. Localized detection of glioma glycolysis using edited ^{1}H MRS. Magn Reson Med 1993;30:18–27.
28. Stejskal EO, Tanner JE. Spin diffusion measurements: Spin echoes in the presence of a time-dependent field gradient. J Chem Phys 1965:42: 288–292.
29. Bandettini PA, Jesmanowicz A, Wang EC, Hyde JS. Processing strategies for time-course data sets in functional MRI of human brain. Magn Reson Med 1993;30:161.
30. Paxinos G, Watson C. The rat brain in stereotaxic coordinates, 3rd ed. San Diego: Academic Press; 1996.
31. Ogawa S, Lee TM, Barrere B. The sensitivity of magnetic resonance image signals of a rat brain to changes in the cerebral venous blood oxygenation. Magn Reson Med 1993;29:205–210.
32. Meyer ME, Yu O, Eclancher B, Grucker D, Chambron J. NMR relaxation rates and blood oxygenation level. Magn Reson Med 1995;34(2):234–241.
33. Barth M, Moser E. Proton NMR relaxation times of human blood samples at 1.5 T and implications for functional MRI. Cell Mol Biol 1997;43:783–791.
34. van As H, Schaaffsma TJ. Flow in nuclear magnetic resonance imaging. In: Petersen SB, Muller RN, Rinck PA, editors. Introduction to biomedical nuclear resonance. New York: Georg Theme Verlag Thieme Inc.; 1985.
35. Thulborn KR, Waterton JC, Mattews PM, Radda GK. Oxygenation dependence of the transverse relaxation time of water protons in whole blood at high field. Biochem Biophys Acta 1982;714:265–270.
36. Grubb J, Raichle ME, Eichling JO, Ter-Pogossian MM. The effects of changes in $PaCO_2$ on cerebral blood volume, blood flow, and vascular mean transit time. Stroke 1974;5:630–639.
37. Le Bihan D, Breton E, Lallemand D, Grenier P, Cabanis E, Laval-Jeantet M. MR imaging of intravoxel incoherent motions: application to diffusion and perfusion in neurologic disorders. Radiology 1986;161:401–407.
38. Lythgoe MF, Busza AL, Calamante F, Sotak CH, King MD, Bingham AC, Williams SR, Gadian DG. Effects of diffusion anisotropy on lesion delineation in a rat model of cerebral ischemia. Magn Reson Med 1997;38(4):662–668.
39. Duong TQ, Silva AC, Lee S-P, Kim S-G. Comparison of spatial localization between synaptic activity and hemodynamic responses following somatosensory stimulation: an MRI study at 9.4 Tesla. In: Proc of the ISMRM 7th Scientific Meeting, Philadelphia, 1999. p 378.